

# Bidirectional Regulation between NDRG1 and GSK3 $\beta$ Controls Tumor Growth and Is Targeted by Differentiation Inducing Factor-1 in Glioblastoma

Hiroshi Ito<sup>1,2</sup>, Kosuke Watari<sup>2</sup>, Tomohiro Shibata<sup>2</sup>, Tomofumi Miyamoto<sup>3</sup>, Yuichi Murakami<sup>2,4</sup>, Yukiko Nakahara<sup>1</sup>, Hiroto Izumi<sup>5</sup>, Hiroaki Wakimoto<sup>6</sup>, Michihiko Kuwano<sup>4</sup>, Tatsuya Abe<sup>1</sup>, and Mayumi Ono<sup>2</sup>



## ABSTRACT

The development of potent and selective therapeutic approaches to glioblastoma (GBM), one of the most aggressive primary brain tumors, requires identification of molecular pathways that critically regulate the survival and proliferation of GBM. Previous studies have reported that deregulated expression of N-myc downstream regulated gene 1 (NDRG1) affects tumor growth and clinical outcomes of patients with various types of cancer including glioma. Here, we show that high level expression of NDRG1 in tumors significantly correlated with better prognosis of patients with GBM. Loss of NDRG1 in GBM cells upregulated GSK3 $\beta$  levels and promoted cell proliferation, which was reversed by selective inhibitors of GSK3 $\beta$ . In contrast, NDRG1 overexpression suppressed growth of GBM cells by decreasing GSK3 $\beta$  levels via proteasomal degradation and by suppressing AKT and S6 cell growth signaling, as well as cell-cycle signaling pathways. Conversely, GSK3 $\beta$  phosphorylated serine and

threonine sites in the C-terminal domain of NDRG1 and limited the protein stability of NDRG1. Furthermore, treatment with differentiation inducing factor-1, a small molecule derived from *Dictyostelium discoideum*, enhanced NDRG1 expression, decreased GSK3 $\beta$  expression, and exerted marked NDRG1-dependent antitumor effects *in vitro* and *in vivo*. Taken together, this study revealed a novel molecular mechanism by which NDRG1 inhibits GBM proliferation and progression. Our study thus identifies the NDRG1/GSK3 $\beta$  signaling pathway as a key growth regulatory program in GBM, and suggests enhancing NDRG1 expression in GBM as a potent strategy toward the development of anti-GBM therapeutics.

**Significance:** This study identifies NDRG1 as a potent and endogenous suppressor of glioblastoma cell growth, suggesting the clinical benefits of NDRG1-targeted therapeutics against glioblastoma.

## Introduction

In 2016, the World Health Organization (WHO) revised the classification of glioma based on the presence of mutations in the *isocitrate dehydrogenase (IDH) 1* and *2* genes and *chromosome 1p/19q* status (1). Glioblastoma (GBM), WHO grade IV and the most common and aggressive primary brain tumor, exhibits a high recurrence rate, and poor prognosis attributable to its invasive nature and resistance to therapy (2). Although abnormal genomic alterations underlying GBM pathogenesis have been discovered (3, 4), genomic

changes that specifically drive the growth and survival of GBM cells remain unclear. Combination of standard therapy, irradiation, and temozolomide, with molecular-targeted drugs, such as EGFR, PI3K, or mTOR inhibitors, failed to improve the overall or progression-free survival in phase III clinical trials (2). The development of effective therapeutic strategies with improved benefits for patients with GBM requires identification of signaling pathways that critically regulate the survival and proliferation of GBM.

N-myc downstream regulated gene 1 (NDRG1) is a member of the NDRG protein family consisting of NDRG1–4, which are evolutionarily well conserved. NDRG1 is a 43 kDa, 394 amino acid protein and predominantly localized in the cytoplasm (5). Initially identified as a differentiation-related gene during embryogenesis, *NDRG1* is inversely correlated with N-myc expression (6) and its mutation is responsible for hereditary motor and sensory neuropathy (7). NDRG1 is intimately involved in multiple stages of differentiation, including placental formation (8), trophoblast formation (9), and maturation of mast cells (10) and macrophage lineage cells (11), as well as in the morphogenesis of various organs (11–13).

NDRG1 suppresses metastasis and oncogenesis in cancers of the brain, breast, colon, esophagus, pancreas, and prostate (5), whereas it promotes tumor growth and metastasis in cancers of the cervix, liver, lung, and stomach (5). We have previously reported that NDRG1 overexpression in pancreatic cancer cells suppresses tumor growth and angiogenesis via attenuation of NF- $\kappa$ B signaling pathway (14–16). In contrast, NDRG1 overexpression in gastric cancer cells promotes tumor growth and angiogenesis through enhanced JNK/AP-1 activation (17). Therefore, NDRG1 is a double-edged sword in human malignancies, and its role and effect could differ depending on tumor types. The precise mechanisms of how NDRG1 regulates tumor malignancy remain unclear.

<sup>1</sup>Department of Neurosurgery, Faculty of Medicine, Saga University, Saga, Japan. <sup>2</sup>Department of Pharmaceutical Oncology, Graduate School of Pharmaceutical Sciences, Kyushu University, Fukuoka, Japan. <sup>3</sup>Department of Natural Products Chemistry, Graduate School of Pharmaceutical Sciences, Kyushu University, Fukuoka, Japan. <sup>4</sup>Cancer Translational Research Center, St. Mary's Institute of Health Sciences, St. Mary's Hospital, Kurume, Japan. <sup>5</sup>Department of Occupational Pneumology, Institute of Industrial Ecological Sciences, University of Occupational and Environmental Health, Kitakyushu, Japan. <sup>6</sup>Department of Neurosurgery, Massachusetts General Hospital, Harvard Medical School, Boston, Massachusetts.

**Note:** Supplementary data for this article are available at Cancer Research Online (<http://cancerres.aacrjournals.org/>).

**Corresponding Author:** Mayumi Ono, Department of Pharmaceutical Oncology, Graduate School of Pharmaceutical Sciences, Kyushu University, 3-1-1 Maidashi, Higashi-ku, Fukuoka, Fukuoka 812-8582, Japan. Phone/Fax: 81-92-642-6296; E-mail: [mono@phar.kyushu-u.ac.jp](mailto:mono@phar.kyushu-u.ac.jp)

Cancer Res 2020;80:234–48

doi: 10.1158/0008-5472.CAN-19-0438

©2019 American Association for Cancer Research.

NDRG1 expression in the nervous system is considerably enhanced during regeneration of injured nerves (18). In neurogenic tumors, higher NDRG1 expression is a favorable prognostic biomarker for patients with neuroblastoma (19). In addition, studies consistently reported that higher NDRG1 expression is correlated with favorable prognosis of patients with gliomas (20, 21). On the other hand, it was reported that NDRG1 bound and stabilized O<sup>6</sup>-methylguanine-DNA methyltransferase (MGMT), which inhibits the function of alkylating agents, and conferred resistance to temozolomide in GBMs (22). Thus, the functional significance of NDRG1 in GBM pathogenesis and patient outcomes remains unclear.

Here, we demonstrate that NDRG1 overexpression induces cell growth suppression and G<sub>0</sub>-G<sub>1</sub> arrest accompanied by reduction of GSK3 $\beta$  expression and inactivation of cell growth signaling pathways. Furthermore, we demonstrate that the differentiation inducing factor-1 (DIF-1) induces a marked enhancement of NDRG1 expression, resulting in tumor growth suppression *in vitro* and *in vivo*. We discuss whether enhancing NDRG1 expression could be a promising approach to the development of potent and novel anti-GBM therapeutics.

## Materials and Methods

### Patient samples and IHC analysis

We analyzed 28 patients who were newly diagnosed as GBM at Saga University Hospital (Saga, Japan) between 2009 and 2016. Clinical status including *IDH1 R132H* mutation and methylation of *MGMT* promoter of the patients is described in Supplementary Table S1. Written informed consent was obtained from all patients or their guardians, and all specimens were collected with the approval of the ethics committee and the Institutional Review Board at the Saga University Hospital (Saga, Japan; approval number: 2017-08-01). This study conforms to the principles of the Declaration of Helsinki. Surgically removed or biopsied GBM specimens were routinely fixed in 20% neutralized formalin and embedded in paraffin. For IHC analysis, 4- $\mu$ m thick sections of a representative block for each tumor were deparaffinized. Heat-induced epitope retrieval was performed with citrate buffer (pH 6.0). The slides were treated with Peroxidase Blocking Solution (S2023; Dako) for 10 minutes to block endogenous peroxidase activity. The slides were then incubated with a primary antibody against NDRG1, which was generated as described previously (1:1,000; ref. 14) for 60 minutes at room temperature. Antibody labeling was achieved using EnVision + Dual Link System HRP (K4061, Dako), and visualized with diaminobenzidine, followed by counterstaining with hematoxylin. NDRG1-positive cells were counted from five high power fields (400 $\times$ ) for each IHC specimen in all patients. All specimens were independently scored for NDRG1 immunopositivity by two observers (H. Ito and Y. Nakahara) blinded to clinical information and the other observer's score.

### Cell culture for GBM cell lines and patient-derived glioma stem-like cells

Human GBM cell lines, U87MG, U251, and T98G were purchased from ATCC and U343 was kindly provided by B. Wetermark (Institute of Pathology, Uppsala, Sweden). 293TN was from System Bioscience. These cells were cultured in DMEM supplemented with 10% FBS. MGG8 and MGG23, human glioma stem-like cell (GSC) lines, were established and characterized at Massachusetts General Hospital (Boston, MA; refs. 23, 24), and cultured in neurobasal medium (Invitrogen) supplemented with L-glutamine (3 mmol/L), B27 supplement (Invitrogen), N2 supplement (Invitrogen), heparin (5  $\mu$ g/mL; Sigma-Aldrich), EGF (20 ng/mL; R&D Systems), and FGF2 (20 ng/mL;

PeproTech). All cell lines were obtained between 1992 and 2015. All cell cultures were maintained at 37°C in a humidified incubator with an atmosphere of 5% CO<sub>2</sub>. All cell lines were passaged for <6 months and were not further tested or authenticated by the authors.

### Antibodies and reagents

Anti-NDRG1 antibody was generated as described previously (1:5,000; ref. 14). Anti-phosphorylated-NDRG1 (Ser330) (1:1,000; 3506), anti-phosphorylated-NDRG1 (Thr346) (1:1,000; D98G11; 5482), anti-phosphorylated-AKT (Thr308) (1:1,000; D25E6; 13038), anti-phosphorylated-AKT (Ser473) (1:2,000; D9E; 4060), anti-AKT (1:1,000; 9272), anti-phosphorylated-S6 kinase (Thr389) (1:1,000; 108D2; 9234), anti-S6 kinase (1:1,000; 9202), anti-phosphorylated-S6 (Ser235/236) (1:2,000; D57.2.2E; 4858), anti-S6 (1:1,000; 5G10; 2217), anti-phosphorylated-GSK3 $\beta$  (Ser9) (1:1,000; D85E12; 5558), anti-GSK3 $\beta$  (1:1,000; 27C10; 9315), anti-phosphorylated-ERK (Thr202/Tyr204) (1:2,000; D13.14.4E; 4370), anti-ERK (1:1,000; 9102), anti-phosphorylated- $\beta$ -catenin (Ser33/37/Thr41) (1:1,000; 9561), anti- $\beta$ -Catenin (1:1,000; 9587), anti-cyclinD1 (1:1,000; 2922), anti-CDK4 (1:1,000; 2906), anti-cyclinE1 (1:1,000; 4129), anti-CDK2 (1:1,000; 2546), and anti-N-myc (1:1,000; 9405) antibodies were purchased from Cell Signaling Technology. Anti- $\alpha$ -tubulin (1:5,000; B-5-1-2; T6074) and anti-FLAG (1:1,000; M2; F1804) antibodies were from Sigma-Aldrich. Anti-glyceraldehyde-3-phosphate dehydrogenase (GAPDH) (1:5,000; 2275-PC-100) antibody was from Trevigen. Anti- $\beta$ -actin (1:5,000; ab8226) antibody was from Abcam. CT99021 (Axon1386) was from Axon Medchem, Tideglusib (S2823) was from Selleck, GSK650394 (3572) was from Tocris Bioscience, and DIF-1 (046-320921) was from FUJIFILM Wako Pure Chemical Corporation. MG132 was from Calbiochem.

### Expression vector construction, transient transfection, and lentiviral transduction

Preparation of the FLAG-tagged NDRG1 and NDRG1 deletion mutants,  $\Delta$ 3- $\Delta$ 6, expression plasmids was as described previously (16). Cells were transfected with pcDNA3-FLAG-NDRG1, pcDNA3-FLAG-NDRG1  $\Delta$ 3- $\Delta$ 6, or pcDNA3 expression plasmids using Lipofectamine LTX (Invitrogen) following the manufacturer's protocol. A FLAG-tagged NDRG1 cDNA was cloned into a lentiviral vector (pCDH-EF1-MCS-BGH-PGK-GFP-T2A-Puro cDNA Cloning and Expression Vector, System Bioscience) for constitutive gene expression. To establish cell lines stably overexpressing NDRG1, U87MG cells were infected with FLAG-tagged NDRG1 cDNA or control lentivirus particles (System Biosciences) for 24 hours. Puromycin (400 ng/mL) was added to select stably transduced cells. Transduction was verified using Western blots.

### Cell growth under NDRG1 silencing

U343 ( $3.5 \times 10^4$  cells), U251 ( $3 \times 10^4$  cells), U87MG ( $2.5 \times 10^4$  cells), and T98G ( $1.75 \times 10^4$  cells) cells were seeded in 24-well plates. The following day, cells were transfected with *NDRG1* or control siRNA (Invitrogen). Cell numbers in each dish were counted by a Z2 Coulter Particle Count and Size Analyzer (Beckman Coulter Inc.) at indicated time points. Triplicate dishes were tested at each day, and results were expressed as the mean  $\pm$  SD of triplicate dishes.

### Cell growth under overexpression of NDRG1 or NDRG1 mutants

U87MG and U251 ( $3.5 \times 10^4$  cells) were seeded in 35-mm dishes. The following day, cells were transfected with FLAG-tagged NDRG1, FLAG-tagged NDRG1 deletion mutants,  $\Delta$ 3- $\Delta$ 6, or vector. U87/mock and U87/NDRG1 sublines (#1, #2, and #3;  $3.5 \times 10^4$  cells) were seeded

Ito et al.

in 35-mm dishes. The cell numbers in each dish were counted by a Z2 Coulter Particle Count and Size Analyzer at indicated time points. Triplicate dishes were tested at each day, and results were expressed as the mean  $\pm$  SD of triplicate dishes.

#### Protein stability assay with cycloheximide

293TN ( $2 \times 10^5$  cells) or U87MG ( $2 \times 10^5$  cells) were seeded in 35-mm dishes. After 48 hours incubation, each dish was treated with DMSO or DIF-1 at 20  $\mu$ mol/L for 24 hours, or after 24 hours incubation, each dish was transfected with mock or *NDRG1* vector for 48 hours. Cycloheximide (06741; Nacalai Tesque) was then added to cells at a concentration of 10  $\mu$ g/mL, and cells were cultured for the indicated times. Cells were harvested and protein levels were visualized by Western blotting with specific antibodies.

#### Sphere formation assay

GSCs ( $3.5 \times 10^4$  cells) were seeded into 24-well plates, incubated for 3 days, and treated with DIF-1 at indicated doses and incubated for another 3 days. Five fields of each well were captured under a 40 $\times$  microscope objective and the diameter of each sphere measured, then the number of spheres that were more than 50  $\mu$ m were counted. Furthermore, from each well, spheres were trypsinized and dyed with trypan blue, and the number of viable cells that excluded trypan blue was counted using TC20 (Bio-Rad).

#### Xenograft studies

Male BALB/c nu/nu athymic nude mice (5–7 weeks old) were purchased from CLEA. For subcutaneous xenograft model,  $5 \times 10^6$  U87MG cells in 200  $\mu$ L of 50% Matrigel were implanted into the subcutaneous tissue of the bilateral abdominal wall of the mice. Tumor sizes were measured, and tumor volumes ( $\text{mm}^3$ ) were calculated as follows: length  $\times$  width<sup>2</sup>  $\times$  0.5. When tumors reached 100–200  $\text{mm}^3$ , 4 mice each were randomly allocated into two groups ( $n$  of evaluable tumors = 6/control group, and  $n = 7$ /DIF-1 treatment group). DIF-1 (300 mg/kg in the morning and 150 mg/kg in the evening, daily) or soybean oil was administered orally twice a day, 6 days/week (25). The tumors were harvested after 11 days, stored at  $-80^\circ\text{C}$ , or fixed immediately in 10% formalin overnight at  $4^\circ\text{C}$ . For orthotopic xenograft model,  $5 \times 10^5$  U87MG cells in 10  $\mu$ L of PBS and  $2 \times 10^5$  MGG8 cells in 5  $\mu$ L of culture medium were stereotactically implanted into the right forebrain of the mice (2 mm lateral from bregma and 2 mm deep). Ten days after implantation, mice were randomly allocated into two groups (U87MG;  $n$  of evaluable tumors;  $n = 3$ /control group, and  $n = 4$ /DIF-1 treatment group; MGG8;  $n$  of evaluable tumors;  $n = 5$ /control group, and  $n = 4$ /DIF-1 treatment group). DIF-1 (300 mg/kg in the morning and 150 mg/kg in the evening, daily) or soybean oil was administered orally twice a day, 6 days/week (25). The right forebrain was harvested after 12 days, fixed immediately in 10% formalin overnight. Formalin-fixed, paraffin-embedded sections were stained with hematoxylin and eosin. To evaluate tumor volumes ( $\text{mm}^3$ ), we measured the maximal area of each tumor, and tumor volume was calculated as: long diameter  $\times$  short diameter<sup>2</sup>  $\times$  0.5. All mice were housed in microisolator cages maintained under a 12 hours light/dark cycle. Water and food were supplied *ad libitum*. Animals were observed for signs of tumor growth, activity, feeding, and pain in accordance with the guidelines of the Harvard Medical Area Standing Committee on Animals. All animal experimental procedures were reviewed and approved by the Animal Ethics Committee of Kyushu University (Fukuoka, Japan; registration number: A30-097-2).

#### DIF-1 distribution into the brain

Male BALB/c nu/nu athymic nude mice (5–7 weeks old) were purchased from CLEA. All mice were randomly allocated into two groups [ $n$  of evaluable plasma and brains for high-performance liquid chromatography (HPLC) and gas chromatography–mass spectrometry (GC–MS) analysis;  $n = 3$ :  $n$  of evaluable brains for Western blot analysis;  $n = 7$ /control group, and  $n = 8$ /DIF-1 treatment group]. For HPLC and GC–MS analysis, DIF-1 (300 mg/kg) or soybean oil was administered orally for 1 hour. For mouse plasma samples, blood samples were collected. Mouse plasma (300  $\mu$ L) was isolated from blood sample by centrifugation at  $500 \times g$  for 15 minutes and was mixed with 300  $\mu$ L chloroform. After mixing, the solution was centrifuged at  $13,000 \times g$  for 5 minutes, and then the organic phase was separated. To prepare brain sample, transcardial perfusion was performed with ice-cold PBS, brain tissues were harvested, and were lysed by sonication in 300  $\mu$ L chloroform. A plasma or brain sample (10  $\mu$ L) was then applied to a column for separation (5C18 Cosmosil AR-II 4.6 I.D.  $\times$  250 mm; Nacalai Tesque). The samples were eluted by a linear gradient of acetonitrile (30%–100%) in the presence of 0.1% formic acid over 40 minutes at a flow rate of 1.0 mL/minute. A UV detector was operated at 277 nm. A calibration curve was prepared by plotting the area ratios of DIF-1 normalized to the internal standard. A plasma or brain sample (10  $\mu$ L) was also subjected to GC–MS [Shimadzu QP-2010SE with INERTCAP 5MS/SIL (0.25 mm inner diameter,  $\times$  30 m), GL Science Inc., column temperature  $100^\circ\text{C}$ – $280^\circ\text{C}$ , rate of temperature increase:  $10^\circ\text{C}/\text{minute}$ ]. For Western blot analysis, DIF-1 (300 mg/kg in the morning and 150 mg/kg in the evening, daily) or soybean oil was administered orally twice a day, 6 days/week. After treatment of DIF-1 for 12 days, the brains were harvested and processed for Western blot analysis.

#### GBM datasets analysis

Data from The Cancer Genome Atlas (TCGA) Research Network (TCGA Glioblastoma Multiforme Provisional complete sample set), including mRNA expressions, mutations, putative copy-number alterations, and clinical data were obtained and analyzed using cBioPortal for Cancer Genomics (<http://www.cbioportal.org>). Data from REMBRANDT datasets and survival information for patients with GBM were obtained and analyzed using Betastasis (<http://www.betastasis.com/glioma/>). Patient prognoses were evaluated by Kaplan–Meier survival curves of patients with GBM with low or high expression of *NDRG1* mRNA expression. In TCGA datasets, patients ( $n = 591$ ) were divided into two groups by  $z$ -score over or less than  $\pm 1.5$ , namely, *NDRG1* low ( $n = 30$ ) and *NDRG1* high ( $n = 22$ ). In REMBRANDT datasets, patients ( $n = 178$ ) were divided into two groups by 50 percentile score of *NDRG1* mRNA expression level, namely, *NDRG1* low ( $n = 89$ ) and *NDRG1* high ( $n = 89$ ).

#### Statistical analysis

The association of *NDRG1*-positive cell rates and overall survival, which was defined by the duration from diagnosis to death, was analyzed by Wilcoxon test and Student  $t$  test. The association of *NDRG1* mRNA level and overall survival was analyzed by Wilcoxon test. Experimental results were expressed as mean  $\pm$  SD (Figs. 2B, D, E, G, 3A and B, 4B, 5C, and H, 6A, C, and E, and 7B, and C; Supplementary Figs. S1A, S1B, S1D, S1E, S1G, S1H, S1I, S2A, S3A, S4A, and S5A) or SEM (Figs. 7A, E, F, and G; Supplementary Fig. S7A) of  $n$  observations. Statistical differences between groups were assessed by two-tailed Student  $t$  test. A  $P$  value of less than 0.05 was considered significant.

## Results

### NDRG1 protein expression correlates with favorable prognosis in patients with GBM

It was previously reported that higher NDRG1 expression in tumors, as assessed by IHC analysis, was predictive of improved prognosis in patients with glioma (20). First, we examined whether NDRG1 expression in tumors correlated with the survival duration of patients with GBM. Surgical samples of 28 newly diagnosed GBMs were IHC analyzed. Representative images of IHC staining of NDRG1 in four clinical samples are shown in **Fig. 1A**. The tumor samples of patients #26 and #27 showed abundant NDRG1 expression, while patients #1 and #8 showed NDRG1 staining in a small subset of cells (**Fig. 1A**), revealing heterogeneity between patients. Kaplan–Meier analysis of overall survival showed that patients with higher NDRG1 expression survived significantly longer than those with lower NDRG1 expression ( $P = 0.004$ ; **Fig. 1B**). Furthermore, the NDRG1-positive cell rates of tumors from all 28 patients positively correlated with longer overall survival of the patients (**Fig. 1C**). These results suggest that NDRG1 expression levels correlate with favorable prognosis in patients with GBM.

### NDRG1 silencing enhances cell growth, GSK3 $\beta$ expression, and cell growth signaling pathway

We examined whether cell growth was affected by altered NDRG1 expression in four GBM cell lines. The cell lines U87MG and U251 harbor loss-of-function *PTEN* mutation, but U343 and T98G do not (26). These GBM cell lines expressed various levels of NDRG1 and cell growth–related signaling molecules; U87MG and U251 had a lower level of NDRG1 and a higher level of pAKT, as compared with U343 and T98 (**Fig. 2A**). It was previously reported that NDRG1 silencing enhanced GBM cell growth accompanied by upregulation of AKT phosphorylation (27). In accord with this study, siRNA-mediated NDRG1 silencing enhanced cell growth of the four GBM cell lines by 1.3- to 2.5-fold (**Fig. 2B**). In particular, U87MG and U251 cells showed more growth enhancement than T98G and U343 cells by NDRG1 silencing (**Fig. 2B**). NDRG1 siRNA markedly suppressed NDRG1 expression in all four GBM cell lines (**Fig. 2C**). In T98G, NDRG1 siRNA did not completely suppress NDRG1 expression, and residual NDRG1 might attenuate the effect of NDRG1 siRNA (**Fig. 2C**). In contrast, in U343 cells, NDRG1 expression was almost completely suppressed by NDRG1 siRNA (**Fig. 2C**). However the effect of siNDRG1 on cell growth was smaller than that of U87MG and

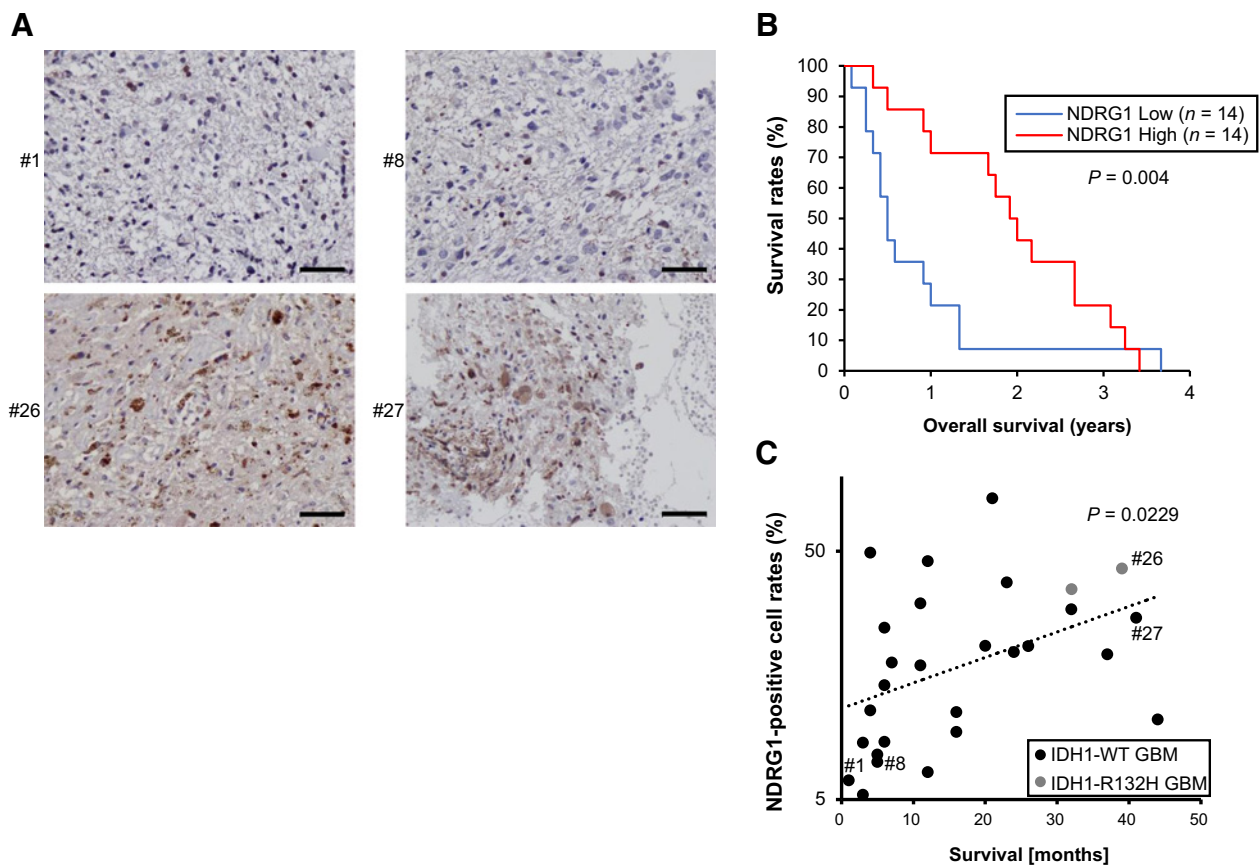
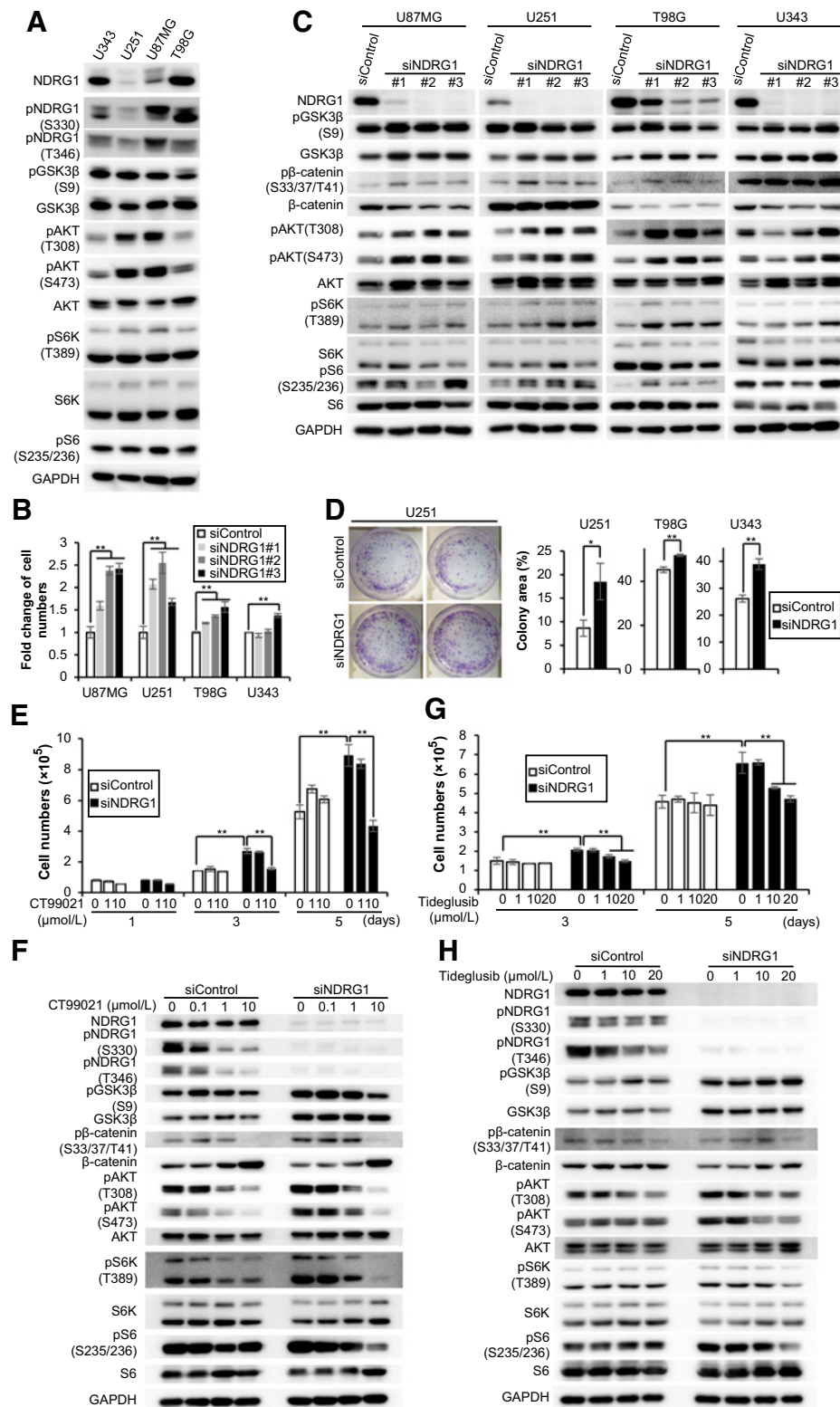


**Figure 1.** NDRG1 expression is correlated with favorable prognosis in patients with GBM. **A**, IHC images of NDRG1 in four surgically resected or biopsied GBM specimens (#1, #8, #26, and #27). Original magnification,  $\times 400$ . Scale bar, 50  $\mu\text{m}$ . **B**, The Kaplan–Meier overall survival analysis based on NDRG1-positive cell rate in patients with GBM. The NDRG1-positive cell rates of tumors from 28 patients were determined as described in Material and Methods. Patients were divided into two groups, namely, NDRG1 low and NDRG1 high, based on 50 percentile score of NDRG1-positive cell rates. Statistical significance was analyzed by Wilcoxon test. **C**, Dot plot analysis of NDRG1-positive cell rates and survival in months. Dotted line, regression line. Statistical significance was analyzed by two-tailed Student *t* test.

Ito et al.



U251 cells. This may be due to the difference of dependency on NDRG1 for cell growth among the cell lines. Interestingly, we found that expression of GSK3 $\beta$  and pGSK3 $\beta$ , as well as pAKT and pS6 was increased upon NDRG1 silencing across these GBM cells (Fig. 2C;

Supplementary Fig. S1A). siNDRG1#3 was selected as siNDRG1 in the following studies. We further examined the effect of NDRG1 silencing on colony formation of U251, T98G, and U343 cell lines, and found that NDRG1 silencing significantly enhanced colony formation of all

three GBM cell lines (Fig. 2D). U87MG could not form colonies. These data suggest that NDRG1 silencing-mediated enhancement of GSK3 $\beta$ , pAKT, and pS6 expression may underlie the observed increases in growth and colony formation.

Next, we examined whether GSK3 $\beta$  activation contributed to NDRG1 silencing-mediated enhancement of cell growth. Treatment with CT99021, a selective ATP competitive GSK3 inhibitor, specifically abrogated NDRG1 silencing-mediated growth enhancement to the control level (Fig. 2E; Supplementary Fig. S1B). In contrast, CT99021 did not significantly alter the growth of control cells (Fig. 2E; Supplementary Fig. S1B). As expected, treatment with CT99021 inhibited  $\beta$ -catenin phosphorylation, which is catalyzed by GSK3 $\beta$  (28). CT99021 also inhibited phosphorylation of AKT (T308 and S473) in both control and NDRG1-silenced cells (Fig. 2F; Supplementary Fig. S1C). Furthermore, CT99021 inhibited phosphorylation of S6K and S6 in both control and NDRG1-silenced cells, but the inhibitory effect of CT99021 was greater in NDRG1-silenced GBM cells than siControl-treated GBM cells (Fig. 2F; Supplementary Fig. S1C and S1D). Moreover, another GSK3 $\beta$  inhibitor, tideglusib, a selective, irreversible, and non-ATP-competitive inhibitor, consistently annihilated cell growth enhancement and suppressed S6K and S6 phosphorylation more in NDRG1-silenced cells than siControl-treated GBM cells (Fig. 2G and H; Supplementary Fig. S1E–S1G). There was no significant effect of CT99021 or tideglusib on total S6K and S6 protein expressions in both control and NDRG1-silenced GBM cells (Supplementary Fig. S1H). These data suggest that GSK3 $\beta$  activation contributes to cell growth enhancement by NDRG1 silencing.

The C-terminal domain of the NDRG1 protein contains several sites for GSK3 $\beta$  and serum and glucocorticoid-regulated kinase (SGK)-mediated phosphorylation (29). We further examined whether SGK activity was also involved in enhanced cell growth after NDRG1 silencing. A competitive SGK inhibitor, GSK650394, suppressed enhanced cell growth by NDRG1 silencing at 1  $\mu$ mol/L (Supplementary Fig. S1I). However, GSK650394 suppressed cell growth and AKT, S6K, and S6 phosphorylation at similar levels in both control and NDRG1-silenced cells (Supplementary Fig. S1I and S1J). Although both GSK3 $\beta$  and SGK inhibitors suppressed cell growth enhanced by NDRG1 silencing, effects of GSK3 $\beta$  inhibitor were more specific in NDRG1-silenced cells. These results suggest the selective involvement of GSK3 $\beta$ , rather than SGK, in NDRG1-dependent cell growth alteration.

#### NDRG1 overexpression suppresses cell growth and GSK3 $\beta$ expression

We next examined the effect of NDRG1 overexpression on cell growth. Transient transfection with exogenous *NDRG1* cDNA induced growth suppression of U87MG and U251 cells (Fig. 3A; Supplementary Fig. S2A). Furthermore, we established three U87/NDRG1 sublines (#1, #2, and #3) via stable overexpression with lentivirus vector transduction, and observed that their growth rates were significantly slower than that of empty vector-transduced U87MG (U87/mock; Fig. 3B). The NDRG1-overexpressing sublines showed reduced levels of GSK3 $\beta$ , p $\beta$ -catenin, pAKT, pS6K, and pS6 expression (Fig. 3C), indicating that NDRG1 overexpression resulted in inactivation of GSK3 $\beta$  and AKT/S6 cell growth signaling pathways. We further found that transient overexpression of NDRG1 in another GBM cell line, U251, also induced inactivation of these signaling molecules (Supplementary Fig. S2B). U87/NDRG1 cells showed an increased cell population at G<sub>0</sub>–G<sub>1</sub>-phase and a decreased cell population at G<sub>2</sub>–M-phase compared with U87/mock cells (Fig. 3D),

indicative of cell-cycle arrest at G<sub>0</sub>–G<sub>1</sub>. NDRG1 overexpression decreased expression of cyclin D1 and E and cyclin-dependent kinase (CDK) 2 and 4 (Fig. 3E). These cyclins (D1 and E) and CDKs (2 and 4) are involved in cell-cycle transition from G<sub>1</sub> to S-phase (30). In addition, we examined the effect of NDRG1 overexpression on cell apoptosis and DNA synthesis by using Annexin V-FITC/propidium iodide (PI) staining assay and bromodeoxyuridine (BrdU) incorporation assay, respectively. NDRG1 overexpression did not alter apoptotic cell (Annexin V-positive) fractions in both U87MG and U251 cells (Supplementary Fig. S2C). In contrast, NDRG1 overexpression inhibited BrdU incorporation in both GBM cell lines, suggesting that NDRG1 overexpression inhibits DNA synthesis (Supplementary Fig. S2D). Together, NDRG1 suppresses GBM cell growth by concomitant downregulation of GSK3 $\beta$ , AKT/S6, and cell-cycle signaling pathways.

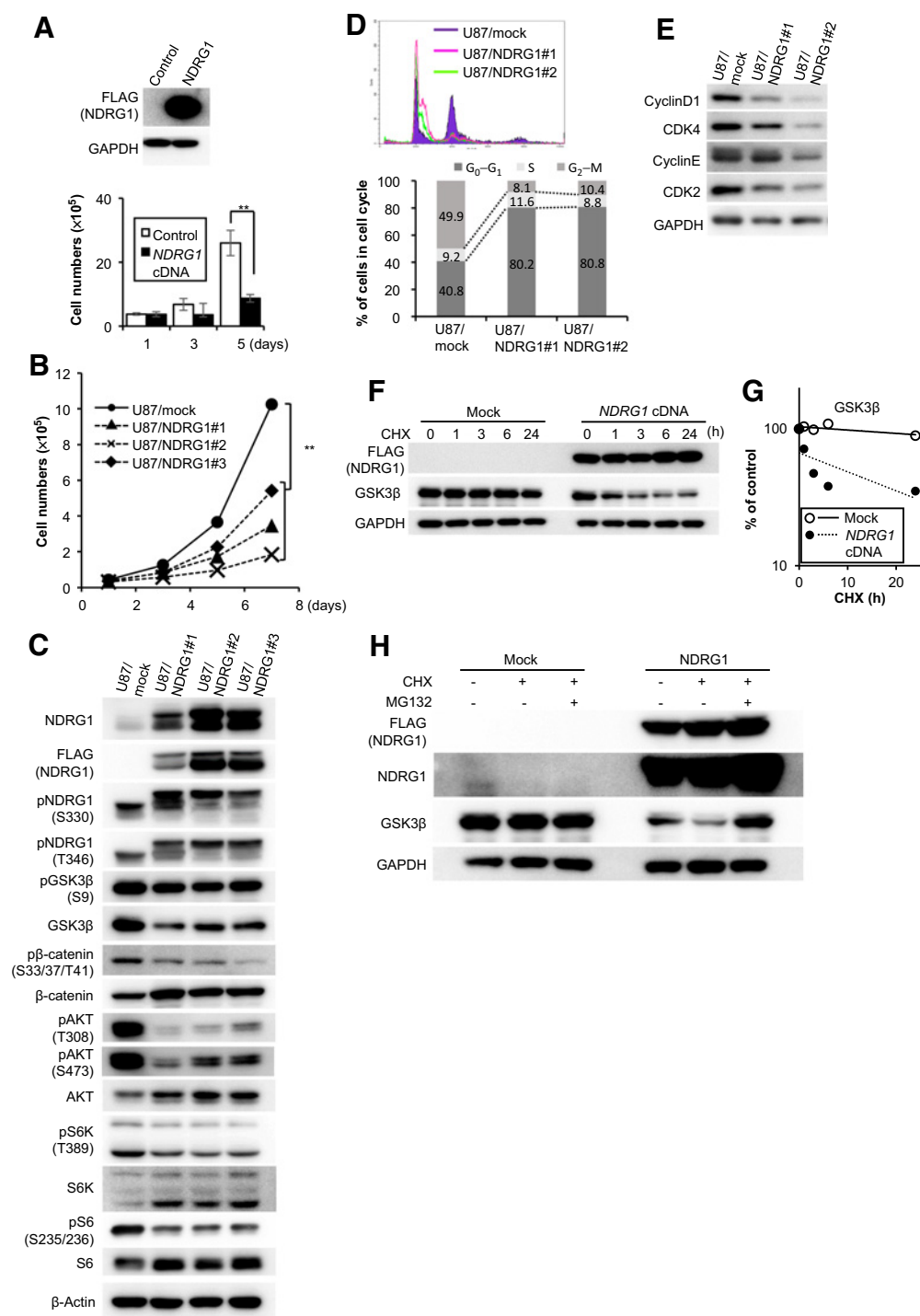
#### NDRG1 reduces GSK3 $\beta$ expression via proteasomal regulation

Furthermore, we determined the mechanism underlying the reduction of GSK3 $\beta$  expression mediated by NDRG1 overexpression. We examined the effect of NDRG1 overexpression on the stability of the GSK3 $\beta$  protein. In the presence of cycloheximide, NDRG1 overexpression destabilized GSK3 $\beta$  with a half-life of approximately 3 hours compared with control cells wherein the GSK3 $\beta$  protein exhibited a half-life of >24 hours, showing its high stability (Fig. 3F and G; Supplementary Fig. S2E). It has previously been reported that a proteasomal inhibitor, MG132, inhibited GSK3 $\beta$  degradation induced by HSP90 inhibitor or dexamethasone (31, 32). Consistent with these studies, the accelerated GSK3 $\beta$  degradation by NDRG1 overexpression was completely blocked by MG132 (Fig. 3H). These data suggested that NDRG1 reduced GSK3 $\beta$  levels by proteasomal degradation pathway.

#### NDRG1 mutants lacking phosphorylation sites facilitate cell growth suppression and protein stabilization

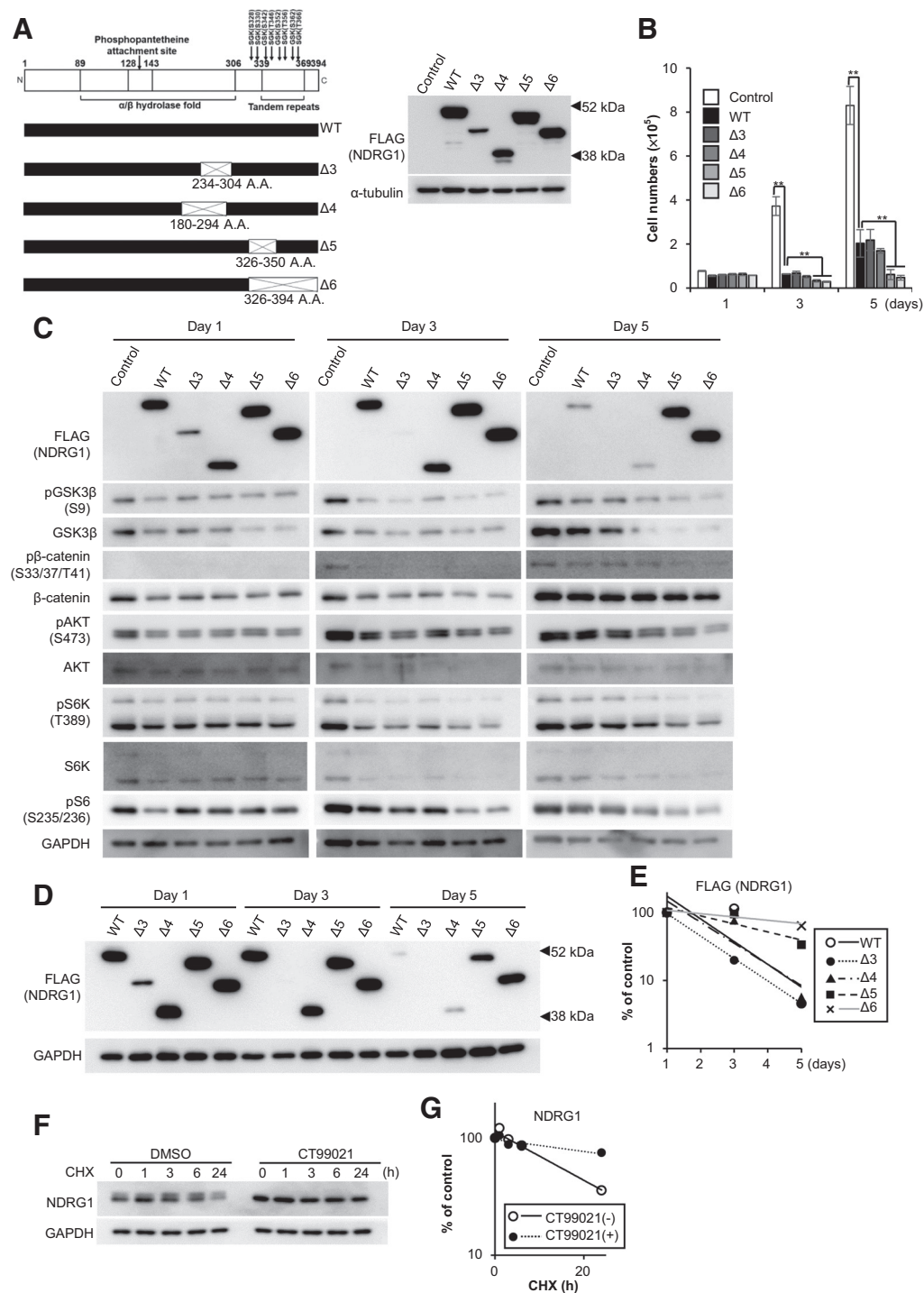
We examined whether a specific domain of NDRG1 was responsible for NDRG1-induced cell growth suppression. Analysis of the amino acid sequence of NDRG1 indicates the presence of a phosphopantetheine attachment, a prominent  $\alpha/\beta$  hydrolase fold, and NDRG1 phosphorylation sites by GSK3 $\beta$  and SGK at its C-terminal domain. We previously established several deletion mutants of NDRG1;  $\Delta$ 3 (234–304AA) and  $\Delta$ 4 (180–294AA) harbor deletions of the partial  $\alpha/\beta$  hydrolase fold, while  $\Delta$ 5 and  $\Delta$ 6 harbor deletions of the partial (326–350AA) and total (326–394AA) phosphorylation sites on the C-terminal domain (Fig. 4A; refs. 16, 29, 33, 34). Transfection of wild-type (WT) and all mutant constructs induced marked cell growth suppression compared with empty vector-transfected control (Fig. 4B). Among the constructs,  $\Delta$ 5 and  $\Delta$ 6 NDRG1 mutants induced the most prominent cell growth suppression (Fig. 4B; Supplementary Fig. S3A), along with reduced GSK3 $\beta$  expression and AKT, S6K, and S6 phosphorylation (Fig. 4C; Supplementary Fig. S3B). Following transfection,  $\Delta$ 5 and  $\Delta$ 6 mutants showed increased NDRG1 protein stability compared with the WT and other mutants (Fig. 4D and E; Supplementary Fig. S3B), suggesting that the C-terminal domain containing GSK3 $\beta$  and SGK phosphorylation sites might be involved in the stability of NDRG1. Indeed, NDRG1 degradation was almost completely blocked by the selective GSK3 inhibitor CT99021 (Fig. 4F and G). Collectively, GSK3 $\beta$ -mediated phosphorylation of NDRG1 negatively regulated the stability of NDRG1. NDRG1 overexpression and its dephosphorylation by GSK3 $\beta$  inhibition effectively suppressed GBM cell growth.

Ito et al.

**Figure 3.**

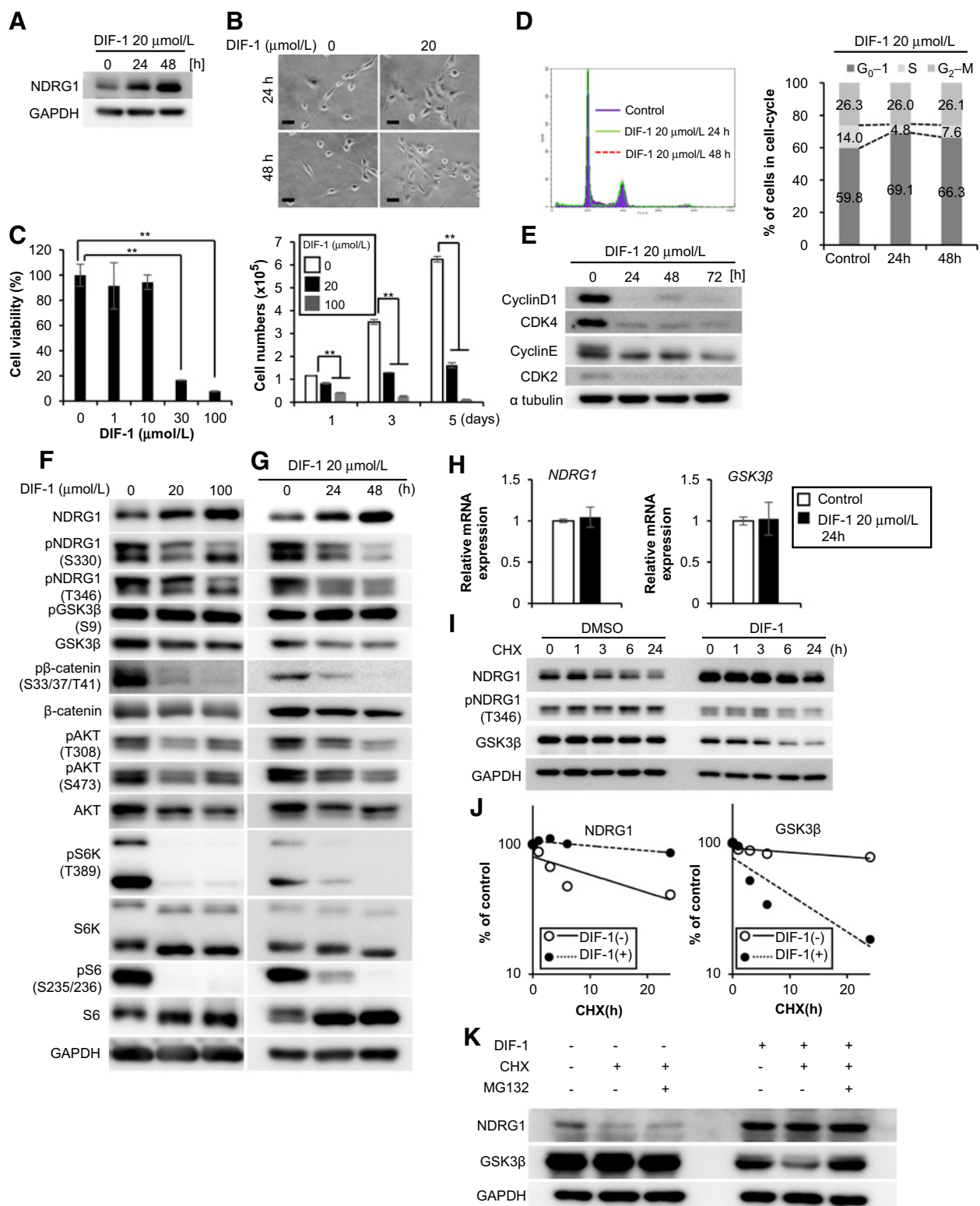
NDRG1 overexpression suppresses cell growth, GSK3 $\beta$  expression, and cell growth and cell-cycle signaling pathways. **A**, Top, Western blot analysis of NDRG1 expression in U87MG cells upon transfection with mock or *NDRG1* cDNA; bottom, cell growth rate of U87MG cells, followed by cDNA-mediated NDRG1 overexpression for indicated duration. **B**, Comparison of cell growth rates between U87/mock and U87/NDRG1 sublines. **C**, Western blot analysis of indicated proteins in U87/mock and U87/NDRG1 sublines. **D**, Flow cytometric analysis of cell cycle in U87/mock and U87/NDRG1 sublines. Top, DNA histogram using FACS; bottom, the percentage of cells in each phase of the cell cycle. **E**, Western blot analysis of cell-cycle-related proteins in U87/mock and U87/NDRG1 sublines. **F** and **G**, Western blot analysis showing GSK3 $\beta$  protein stability in the presence of 10  $\mu$ g/mL cycloheximide (CHX) after 24 hours from transfection of mock or *NDRG1* cDNA in 293TN cells (**F**) and degradation curves for GSK3 $\beta$  normalized to the expression levels at 0 hour (**G**). **H**, Western blot analysis showing NDRG1 and GSK3 $\beta$  protein expression. 293TN cells were transfected with mock or *NDRG1* cDNA for 24 hours, followed by treatment with 10  $\mu$ g/mL cycloheximide and/or 10  $\mu$ mol/L MG132 for 6 hours. Error bars,  $\pm$  SD of triplicate dishes; two-tailed Student *t* test. \*\*,  $P < 0.01$ .

## NDRG1 Suppresses Glioblastoma

**Figure 4.**

WT and various mutants of NDRG1 exert differential inhibitory effects on cell growth. **A**, Left, a schematic representation of NDRG1 deletion mutants. Right, Western blot analysis indicating WT and mutant NDRG1 expression 48 hours after transfection of the indicated vectors in U87MG cells. **B**, The inhibitory effects of WT and the four deletion mutants of NDRG1 on cell growth in U87MG. Cells were transfected with cDNA of WT or various NDRG1 constructs for 24 hours and monitored for cell growth for indicated duration. Error bars,  $\pm$  SD of triplicate dishes; two-tailed Student *t* test; \*\*,  $P < 0.01$ . **C**, Western blot analysis showing the effects of WT and four deletion mutants of NDRG1 on cell signaling molecules. U87MG cells were transfected with cDNA of various NDRG1 constructs and cell lysates prepared at indicated days following cDNA transfection. **D** and **E**, Western blot analysis showing the stability of WT and four deletion mutants of NDRG1 following the transfection of the corresponding constructs in U87MG cells (**D**) and degradation curves for exogenous FLAG-tagged NDRG1 normalized to each expression at day 1 (**E**). **F** and **G**, Western blot analysis showing the stability of NDRG1 protein in the presence of cycloheximide (CHX) with or without CT99021 (10  $\mu$ mol/L) for 24 hours in 293TN cells (**F**) and degradation curves for NDRG1 normalized to each expression levels at 0 hour (**G**).

Ito et al.

**Figure 5.**

DIF-1 suppresses GBM cell growth and enhances NDRG1 expression levels. **A**, The effect of DIF-1 on NDRG1 expression in U87MG cells. Cells were exposed to 20  $\mu\text{mol/L}$  DIF-1 for indicated duration, followed by Western blot analysis. **B**, Representative microscopic images of U87MG cell morphology upon treatment with DIF-1 for 24 or 48 hours. Original magnification,  $\times 200$ . Scale bar, 50  $\mu\text{m}$ . **C**, The effect of DIF-1 on cell growth of U87MG. Left, cells were exposed to various concentrations of DIF-1 for 72 hours; right, cells were exposed to the indicated concentrations of DIF-1 for indicated duration. (Continued on the following page.)

### DIF-1 increased NDRG1 expression, decreased GSK3 $\beta$ expression, and suppressed GBM cell growth

DIF-1 was identified in *Dictyostelium discoideum* as a putative morphogen required for differentiation of stalk cells (35). The anti-tumor effects of DIF-1 including *in vivo* antimetastatic effects have been reported in close context with Wnt/ $\beta$ -catenin signaling pathway (25, 36). Given the physiologic roles that NDRG1 plays in differentiation (8–11), we hypothesized that DIF-1 might alter NDRG1 signaling.

DIF-1 markedly increased NDRG1 expression in a time-dependent manner in U87MG cells (Fig. 5A), accompanied with morphologic transition from fibroblastic to a round shape and cell–cell adherent characteristic (Fig. 5B). Furthermore, DIF-1 inhibited cell growth (Fig. 5C), and flow cytometric analysis demonstrated that DIF-1 induced cell growth arrest at G<sub>0</sub>–G<sub>1</sub>-phase (Fig. 5D). DIF-1 suppressed cyclin D1, cyclin E, CDK4, and CDK2 expression in a time-dependent manner (Fig. 5E). Consistent with these data, DIF-1 increased NDRG1 expression and inhibited cell growth in another GBM cell line, U251 (Supplementary Fig. S4A and S4B). Furthermore, DIF-1 decreased GSK3 $\beta$  levels and suppressed phosphorylation of AKT, S6K, S6, and  $\beta$ -catenin in a dose- and time-dependent manner (Fig. 5F and G; Supplementary Fig. S4B). We next examined the effect of DIF-1 on cell apoptosis and DNA synthesis by using Annexin V-FITC/PI staining assay and BrdU incorporation assay, respectively. Treatment with DIF-1 did not alter apoptotic cell (Annexin V-positive) fractions in both U87MG and U251 cells (Supplementary Fig. S4C). In contrast, DIF-1 markedly decreased BrdU incorporation in both GBM cell lines, suggesting that DIF-1 inhibits DNA synthesis (Supplementary Fig. S4D). DIF-1 induced an increase in NDRG1 and a decrease in GSK3 $\beta$  levels without affecting the mRNA levels of these genes (Fig. 5H). We next examined the effect of DIF-1 on the stability of NDRG1 and GSK3 $\beta$  proteins. Compared with DMSO control, DIF-1 consistently enhanced NDRG1 expression levels and decreased pNDRG1 and GSK3 $\beta$  expression levels (Fig. 5I; Supplementary Fig. S4E). NDRG1 degraded with a half-life of >24 hours and approximately 6 hours in DIF-1-treated cells and control cells, respectively (Fig. 5I and J; Supplementary Fig. S4E). In contrast, DIF-1 considerably destabilized GSK3 $\beta$  with a half-life of approximately 3 hours compared with control cells, wherein the GSK3 $\beta$  protein exhibited a half-life of >24 hours (Fig. 5I and J; Supplementary Fig. S4E). The accelerated GSK3 $\beta$  degradation by DIF-1 was abrogated by MG132 (Fig. 5K), suggesting the involvement of proteasomal degradation in DIF-1-induced downregulation of GSK3 $\beta$ . However, NDRG1 degradation in untreated control cells was not recovered by MG132 (Fig. 5K).

### NDRG1 silencing blunted DIF-1-induced cell growth suppression

Furthermore, we examined whether NDRG1 silencing affected the effects of DIF-1 on cell growth and downstream signaling. NDRG1 silencing counteracted the cell growth suppression caused by DIF-1 (Fig. 6A; Supplementary Fig. S5A). DIF-1 did not upregulate NDRG1 in the presence of siNDRG1 (Fig. 6B; Supplementary Fig. S5B). DIF-1

suppressed GSK3 $\beta$  and pAKT expression, which was reversed when NDRG1 was silenced (Fig. 6B; Supplementary Fig. S5B). Decreased phosphorylation of S6K and S6, however, was observed in both control and NDRG1-silenced cells exposed to DIF-1 (Fig. 6B; Supplementary Fig. S5B). We further examined whether GSK3 $\beta$  overexpression specifically rescued DIF-1-induced cell growth suppression of GBM cells. Transient transfection of exogenous GSK3 $\beta$  cDNA significantly annihilated DIF-1-induced cell growth suppression (Fig. 6C). Collectively, these results indicate that DIF-1-induced upregulation of NDRG1 and downregulation of GSK3 $\beta$  drive modulation in downstream signaling, leading to cell growth suppression in GBM.

### DIF-1 suppresses sphere formation by GSCs

Next, we examined whether DIF-1 could suppress cell growth in patient-derived GSCs (MGG8 and MGG23), which were cultured under glioma sphere culture conditions to maintain the original phenotypes and genotypes (24, 37, 38). DIF-1 suppressed both sphere formation and cell growth of MGG8 and MGG23 in a dose-dependent manner under sphere culture conditions (Fig. 6D and E). Moreover, DIF-1 enhanced NDRG1 expression, and suppressed expression of pNDRG1 (S330), GSK3 $\beta$ , p $\beta$ -catenin, pAKT, pS6K, S6K, and pS6, as well as several tested cell-cycle-related proteins (Fig. 6F). Furthermore, DIF-1 suppressed N-myc expression in MGG8 cells that harbor MYCN amplification (Fig. 6F).

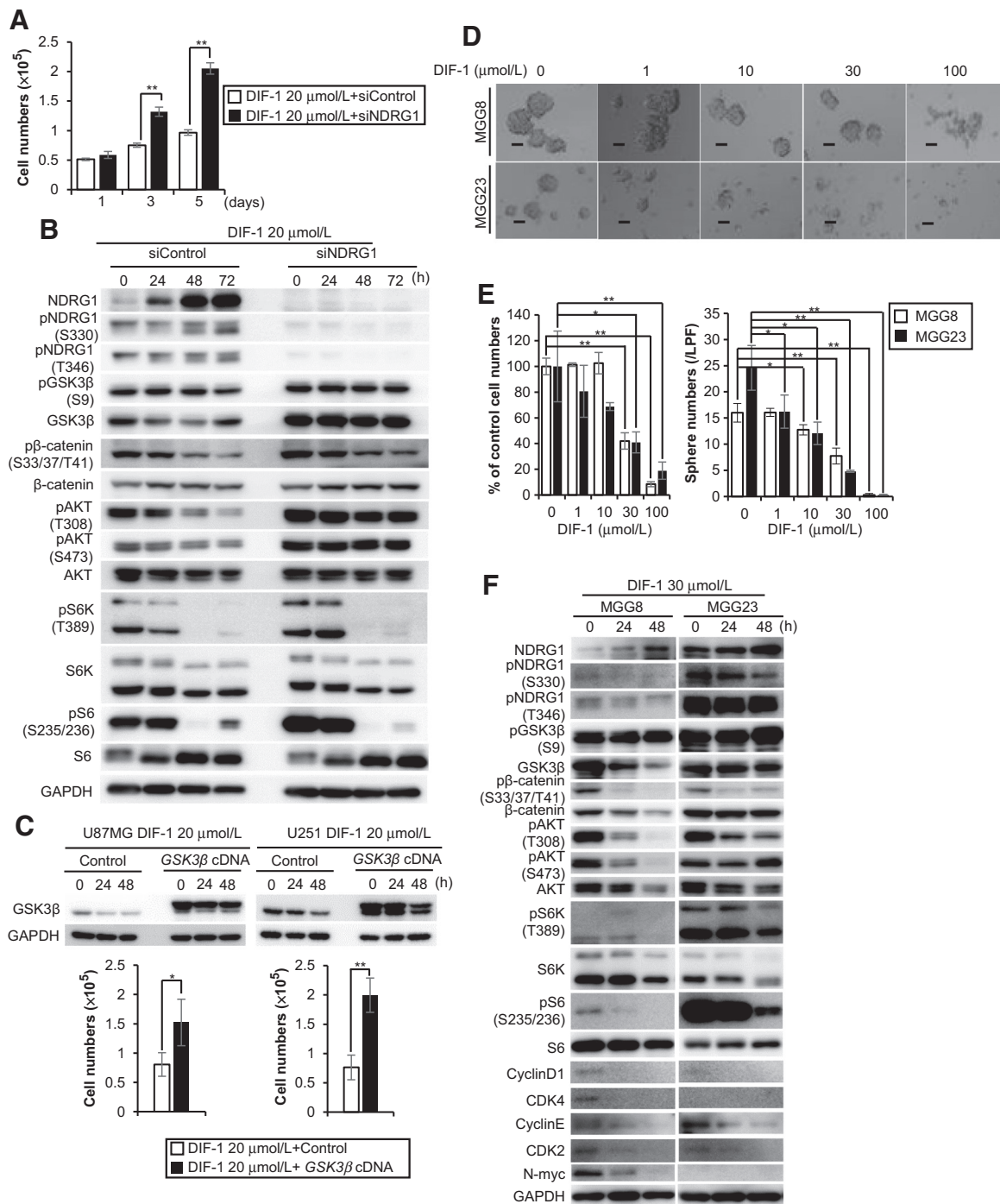
### DIF-1 suppresses GBM tumor growth *in vivo*

Finally, we determined the antitumor effects of DIF-1 in xenograft therapeutic models *in vivo*. Oral administration of DIF-1 suppressed tumor growth in both volume ( $P < 0.05$ ) and weight ( $P = 0.069$ ) in a U87MG subcutaneous xenograft model (Fig. 7A and B). No difference in body weight was observed between control and DIF-1-treated mice (Fig. 7C). NDRG1 expression levels were higher and pNDRG1 expression levels were lower in DIF-1-treated tumors ( $n = 7$ ) when compared with control tumors ( $n = 6$ ; Fig. 7D). GSK3 $\beta$  expression levels were lower in DIF-1-treated tumors than in control tumors; moreover, phosphorylation of  $\beta$ -catenin, AKT, and S6 was decreased following treatment with DIF-1 (Fig. 7D).

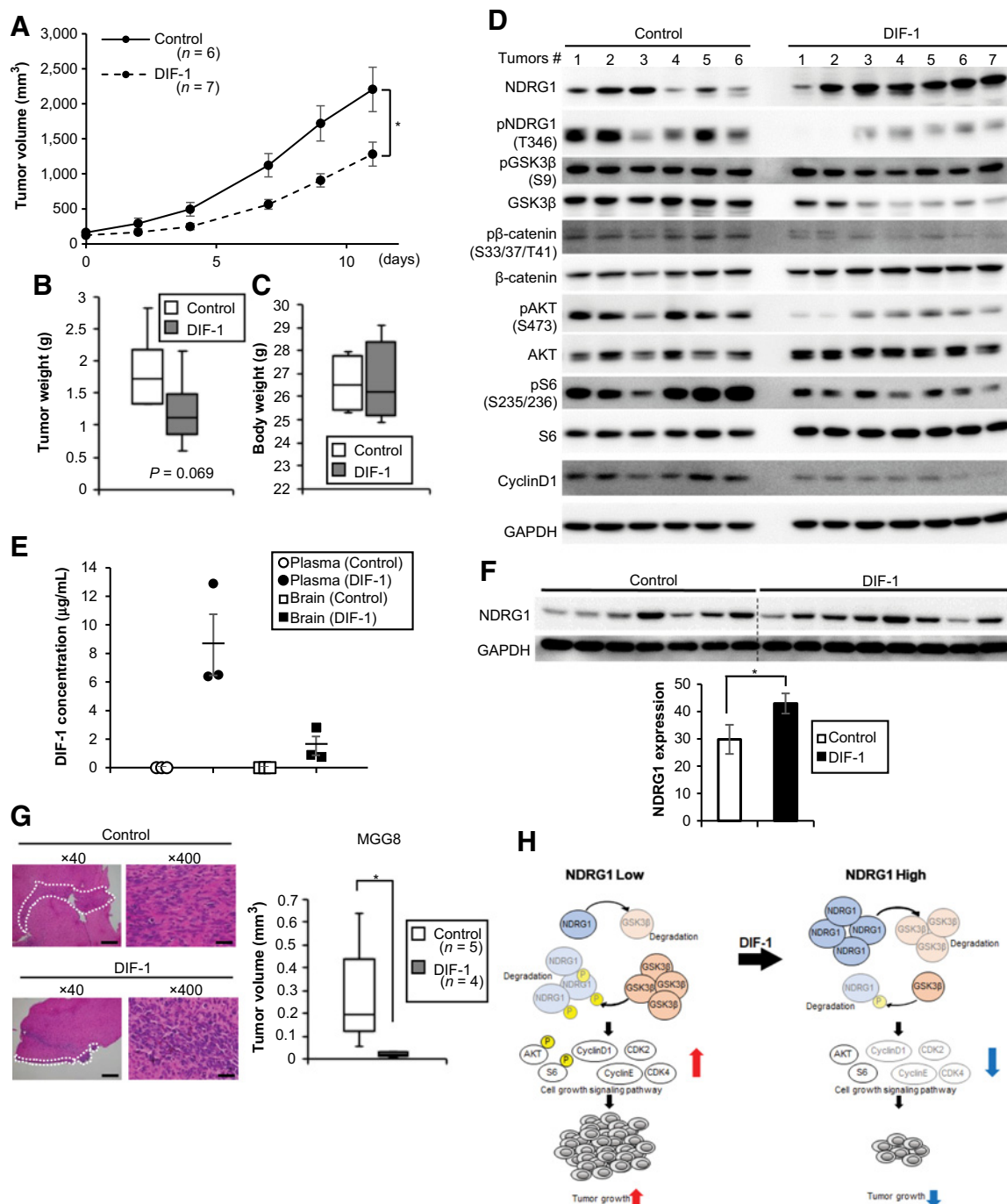
We next examined the ability of DIF-1 to penetrate the blood–brain barrier (BBB) by HPLC and GC–MS analyses. It was previously reported that HPLC analysis determined the plasma levels of DIF-1 at 1 hour after single oral administration of DIF-1 (25). Our HPLC analysis demonstrated that DIF-1 was detected at  $8.58 \pm 2.15 \mu\text{g/mL}$  in plasma ( $n = 3$ ), and at  $1.48 \pm 0.66 \mu\text{g/mL}$  ( $n = 3$ ) in the brain at 1 hour after single oral administration of DIF-1 (300 mg/kg; Fig. 7E; Supplementary S6A). GC–MS analysis also detected the base peak ( $m/z = 201$ , C<sub>9</sub>H<sub>10</sub><sup>35</sup>ClO<sub>3</sub>) corresponding to DIF-1 in the brain as well as in plasma after oral administration of DIF-1 (Supplementary Fig. S6B). We further found that NDRG1 expression levels were relatively higher in DIF-1-treated brain tissues ( $n = 8$ ) than untreated control brain tissues ( $n = 7$ ; Fig. 7F). These data strongly suggested that DIF-1 was able to cross the BBB and distribute into the brain. Next, we examined the antitumor effects of DIF-1 in orthotopic MGG8 and

(Continued.) **D**, Flow cytometric analysis of cell cycle in U87MG cells treated with 20  $\mu\text{mol/L}$  DIF-1. Left, DNA histogram by FACS; right, the percentage of cells in each phase of the cell cycle. **E**, Western blot analysis of cell-cycle-related proteins in U87MG cells treated with 20  $\mu\text{mol/L}$  DIF-1 for indicated duration. **F** and **G**, Effect of DIF-1 on NDRG1 and downstream effector expression. **F** and **G**, Cells were exposed to the indicated concentrations of DIF-1 for 24 hours (**F**) or to 20  $\mu\text{mol/L}$  DIF-1 for indicated duration (**G**), followed by Western blot analysis. **H**, qRT-PCR analysis of *NDRG1* and *GSK3 $\beta$*  mRNA expression in U87MG cells with or without 20  $\mu\text{mol/L}$  DIF-1 for 24 hours. **I** and **J**, Western blot analysis showing NDRG1 and GSK3 $\beta$  protein stability in the presence of 10  $\mu\text{g/mL}$  cycloheximide (CHX) for 24 hours following mock or DIF-1 (20  $\mu\text{mol/L}$ ) treatment in 293TN cells (**I**) and degradation curves for NDRG1 and GSK3 $\beta$  normalized to each expression level at 0 hour (**J**). **K**, Western blot analysis showing NDRG1 and GSK3 $\beta$  protein expression. 293TN cells were treated with or without DIF-1 for 24 hours, followed by treatment with 10  $\mu\text{g/mL}$  cycloheximide and/or MG132 at 10  $\mu\text{mol/L}$  for 6 hours. Error bars,  $\pm$  SD of triplicate dishes; two-tailed Student *t* test. \*\*,  $P < 0.01$ .

Ito et al.

**Figure 6.**

DIF-1 suppressed GBM cell growth by enhancing NDRG1 expression. **A**, Comparison of the inhibitory effect of DIF-1 on cell growth between control and NDRG1-silenced U87MG cells. Cells were treated with control or *NDRG1* siRNA for 24 hours and cell growth was followed with DIF-1 for indicated duration. **B**, Western blot analysis of control and NDRG1-silenced U87MG cells treated with 20  $\mu\text{mol/L}$  DIF-1. Cells were treated with siRNA for 24 hours and further incubated with 20  $\mu\text{mol/L}$  DIF-1 for indicated duration. **C**, Top, Western blot analysis of GSK3 $\beta$  expression in U87MG and U251 cells upon transfection with mock or *GSK3 $\beta$*  cDNA; bottom, comparison of the inhibitory effect of DIF-1 on cell growth between control and GSK3 $\beta$ -overexpressed U87MG and U251 cells. Cells were transfected with control or *GSK3 $\beta$*  cDNA for 24 hours and cell growth was followed with 20  $\mu\text{mol/L}$  DIF-1 for 3 days. **D**, Effects of DIF-1 on sphere formation by MGG8 and MGG23 cells. Representative images of counted spheres are shown. Original magnification,  $\times 40$ . Scale bar, 50  $\mu\text{m}$ . **E**, Left, effects of DIF-1 on cell growth and sphere formation by MGG8 and MGG23 cells. Cells were exposed to various concentrations of DIF-1 for 72 hours and viable cells were counted; right, spheres  $> 50 \mu\text{m}$  in size were counted. **F**, Western blot analysis of the effects of DIF-1 (30  $\mu\text{mol/L}$ ) on NDRG1 and downstream effectors in MGG8 and MGG23 cells. Error bars,  $\pm$  SD of triplicate dishes; two-tailed Student *t* test. \*,  $P < 0.05$ ; \*\*,  $P < 0.01$ .

**Figure 7.**

DIF-1 suppresses tumor growth by GBM cells in both subcutaneous and orthotopic therapeutic models. **A**, Tumor growth of U87MG cells after treatment with soybean oil (control) or DIF-1 in a mouse xenograft experiment for 11 days. Administration of DIF-1 was initiated when tumors reached a size of 100–200 mm<sup>3</sup>. **B** and **C**, Tumor weight (**B**) of U87MG tumors and body weight (**C**) of each mouse after 11 days of treatment with soybean oil (n = 6) or DIF-1 (n = 7). **D**, Western blot analysis of control and DIF-1-treated U87MG tumors after 11 days of treatment. **E**, Dot plot shows the concentration of DIF-1 in mouse plasma and brain samples (n = 3) after 1 hour of single oral administration of DIF-1 (300 mg/kg). Error bars, ± SEM of each sample. **F**, Top, Western blot analysis of normal brain in control and DIF-1-treated mice. Bottom, protein expression levels of NDRG1 in control and DIF-1-treated brains. Error bars, ± SEM of each brain. **G**, Representative images of hematoxylin and eosin-stained section of tumors in MGG8 orthotopic xenografted mice. Original magnification, ×40 and ×400. Scale bar, 50 μm and 500 μm, respectively. Box plot shows tumor volumes of control mice and DIF-1-treated mice. Error bars, ± SEM of each tumor. **H**, Mechanistic model of the NDRG1/GSK3β signaling pathways in GBM. Left, in tumors that express low levels of NDRG1, GSK3β protein is stabilized and is then highly expressed in tumor, resulting in cell growth signaling pathways and tumor growth. High level GSK3β phosphorylates NDRG1 and retains intracellular NDRG1 low level. Right, DIF-1 treatment induces NDRG1 stabilization and promotes proteasomal degradation of GSK3β, which suppresses cell growth signaling pathways and tumor growth. Two-tailed Student *t* test; \*, *P* < 0.05.

Ito et al.

U87MG GBM xenograft models. In these orthotopic therapeutic models, oral administration of DIF-1 induced tumor growth suppression of MGG8 cells ( $P < 0.05$ ) and U87MG cells ( $P = 0.098$ ; **Fig. 7G**; Supplementary Fig. S7A).

## Discussion

In this study, we studied the effects of NDRG1 on GBM cell growth using NDRG1 silencing and overexpression, and showed that NDRG1 suppresses GBM cell growth through decreased GSK3 $\beta$  expression together with AKT and S6 inactivation. Furthermore, NDRG1 induced cell growth arrest at G<sub>0</sub>-G<sub>1</sub> cell-cycle phase.

This work demonstrated that GSK3 $\beta$  is critically involved in NDRG1-dependent growth regulation in GBM. NDRG1 is an intrinsic cell growth suppressor of GBM through suppression of GSK3 $\beta$  expression via accelerated degradation, followed by suppression of AKT/S6 cell growth signaling and cell-cycle pathways (**Fig. 7H**). It is well known that GSK3 $\beta$  phosphorylation at its N-terminal serine residue by AKT inactivates GSK3 $\beta$  (39), and historically, GSK3 $\beta$  has been considered as a tumor suppressor due to its ability to phosphorylate protooncogenic molecules, c-Myc, cyclinD1, and  $\beta$ -catenin, targeting them for proteasomal degradation (40). On the other hand, there is increasing evidence that GSK3 $\beta$  acts as a positive regulator of cancer cell proliferation and contributes to unfavorable prognosis in various cancers (41). Indeed, it was reported that GSK3 $\beta$  positively regulated the PI3K/AKT/mTOR signaling pathway by phosphorylating AKT and inhibiting PTEN and TSC2 (39). In GBM, GSK3 $\beta$  is now considered to promote invasion, tumorigenesis, and resistance to therapy (42, 43). These observations on protumorigenic functions of GSK3 $\beta$  are in accord with our finding that suppression of GSK3 $\beta$  is the main molecular mechanism of NDRG1 suppression of GBM.

NDRG1 contains Thr/Ser sites at its C-terminal domain that are targeted by GSK3 $\beta$  and SGK for phosphorylation (see **Fig. 4A**; refs. 16, 29, 33, 34). In this study, we revealed that deletion mutants lacking the phosphorylation domain exhibited extended protein stability and mediated more prominent suppression of cell growth, GSK3 $\beta$  expression, and cell growth signaling. Consistent with a previous study (44), the GSK3 $\beta$  inhibitor, CT99021, inhibited NDRG1 phosphorylation and stabilized NDRG1. These results indicated that NDRG1 and GSK3 $\beta$  negatively regulated each other's protein expression by promoting degradation or instability. Although our work supports a vital role of GSK3 $\beta$  in phosphorylation and destabilization of NDRG1, proteasome inhibitor MG132 did not rescue NDRG1 degradation, suggesting mechanisms independent of the proteasome. Further studies are required to understand the mechanisms underlying how the NDRG1 protein degrades in GBM cells and how NDRG1 phosphorylation connects to its degradation. Furthermore, we determined whether GSK3 $\beta$  and/or SGK are essential for GBM cell growth driven by NDRG1 loss. Treatment with GSK3 $\beta$  inhibitor, CT99021 or tideglusib, selectively suppressed the cell growth enhancement and cell growth signaling activated by NDRG1 silencing. The SGK inhibitor, GSK650394, on the other hand, suppressed cell growth and signaling activation regardless of NDRG1 status. These NDRG1-selective effects of GSK3 $\beta$  support a crucial role that GSK3 $\beta$  plays in GBM cell growth promoted by NDRG1 loss. However, further studies are necessary to understand the specific role of SGK and GSK3 $\beta$  in NDRG1 loss-accelerated cell growth in connection with NDRG1 phosphorylation status.

Concerning prognostic significance of NDRG1 in patients with GBM, current (**Fig. 1**) and previous (20, 21) studies demonstrated that

NDRG1 protein expression levels consistently correlated with longer survival. However, microarray data obtained from TCGA and REMBRANDT datasets (45, 46) showed that there is no significant correlation between NDRG1 mRNA levels and overall survival in patients with GBM (Supplementary Fig. S8A). This apparent discrepancy may indicate that protein levels rather than transcript levels better reflect the biological functions of NDRG1 in GBM.

DIF-1 has previously been reported to exhibit an inhibitory effect on cancer cell growth through inactivation of the Wnt/ $\beta$ -catenin signaling pathway and resulting reduction of cyclin D1 and c-Myc expression levels (25, 36, 47). This study demonstrates a novel mechanism of DIF-1 and its antitumor effects in GBM (**Fig. 7H**). DIF-1 potently enhanced NDRG1 protein levels, suggesting protein stabilization as a mechanism of DIF-1-induced NDRG1 upregulation (**Fig. 7H**). DIF-1 also accelerated degradation of GSK3 $\beta$  in a NDRG1-dependent manner, followed by inactivation of the AKT/S6 cell growth signaling pathways (**Fig. 7H**). Of note, DIF-1-induced growth suppression was significantly overcome by NDRG1 silencing, followed by a considerable restoration of GSK3 $\beta$  and pAKT expression. These data strongly suggest that DIF-1-induced NDRG1 upregulation directly mediated cell growth suppression. However, DIF-1 suppression of S6K and S6 phosphorylation was not recovered by NDRG1 silencing, indicating the presence of DIF-1 effects that are NDRG1 independent. Therefore, multiple mechanisms likely underlie DIF-1 antitumor effects, including enhancement of NDRG1 expression, inhibition of S6K/S6 phosphorylation, and other previously reported mechanisms. Finally, *in vivo* tumor growth of GBM cells was suppressed by DIF-1. Our *in vitro* and *in vivo* data consistently demonstrated that enhancement of NDRG1 expression, inhibition of GSK3 $\beta$  and NDRG1 phosphorylation, and inactivation of cell growth signaling pathways characterized the cell signaling effects of DIF-1 (**Fig. 7H**).

In addition, DIF-1 inhibited N-myc expression in MGG8 cells that harbor MYCN amplification (24, 38). The *myc* family of genes including MYCN, drive the development of nervous system and hematologic tumors (48), and NDRG1 was initially identified as a gene downregulated by N-myc or c-Myc (49). The *myc* gene is reportedly amplified in 4% of GBMs (4) and contributes to the maintenance of GBM cancer stem cells (50). The unique effects of DIF-1 on N-myc suppression and enhanced NDRG1 expression may contribute to the elimination of GBM stem cells.

We found that DIF-1 could cross the BBB and distribute into brain (**Fig. 7E**; Supplementary Fig. S6A and S6B), and oral administration of DIF-1 suppressed GBM tumor growth in both subcutaneous and orthotopic therapeutic models (**Fig. 7A, B and G**; Supplementary Fig. S7A). Furthermore, oral administration of DIF-1 induced its penetration through the BBB, enhanced the expression of NDRG1 in brain tissues, and inhibited GBM growth in the brain. Despite such encouraging anti-GBM effects of DIF-1 we showed *in vitro* and *in vivo*, its development as a novel therapeutic agent for GBM, and potentially other cancer, requires pharmacologic optimization. The half-life of DIF-1 in plasma concentration is shorter than 12 hours (25). In addition, high dose administration of DIF-1 was required to suppress tumor growth of GBM. Using DIF-1 as a prototype, development of derivative agents that have improved pharmacokinetics properties such as stability in the blood will allow clinical application of DIF-1-related compounds for cancer therapy.

In conclusion, we show that NDRG1 is a potent tumor suppressor in GBM. The bidirectional regulation of NDRG1 and GSK3 $\beta$  that we discovered herein represents an attractive therapeutic target for GBM. Agents that upregulate NDRG1 like DIF-1 could contribute to the development of potent therapeutic strategies against GBM.

**Disclosure of Potential Conflicts of Interest**

No potential conflicts of interest were disclosed.

**Authors' Contributions**

**Conception and design:** H. Ito, K. Watari, M. Kuwano, M. Ono

**Development of methodology:** K. Watari

**Acquisition of data (provided animals, acquired and managed patients, provided facilities, etc.):** H. Ito, K. Watari, T. Shibata, Y. Murakami, Y. Nakahara

**Analysis and interpretation of data (e.g., statistical analysis, biostatistics, computational analysis):** H. Ito, T. Miyamoto, H. Wakimoto

**Writing, review, and/or revision of the manuscript:** H. Ito, K. Watari, Y. Murakami, H. Wakimoto, M. Kuwano, M. Ono

**Administrative, technical, or material support (i.e., reporting or organizing data, constructing databases):** H. Izumi, M. Ono

**Study supervision:** M. Kuwano, T. Abe

**Acknowledgments**

This research was supported by JSPS KAKENHI grant number JP17K07169 (K. Watari) and by St. Mary's Institute of Health Sciences (M. Ono).

The costs of publication of this article were defrayed in part by the payment of page charges. This article must therefore be hereby marked *advertisement* in accordance with 18 U.S.C. Section 1734 solely to indicate this fact.

Received February 5, 2019; revised June 4, 2019; accepted November 7, 2019; published first November 13, 2019.

**References**

- Louis DN, Perry A, Reifenberger G, von Deimling A, Figarella-Branger D, Cavenee WK, et al. The 2016 World Health Organization classification of tumors of the central nervous system: a summary. *Acta Neuropathol* 2016;131:803–20.
- Geraldo LHM, Garcia C, da Fonseca ACC, Dubois LGF, de Sampaio E Spohr TCL, et al. Glioblastoma therapy in the age of molecular medicine. *Trends Cancer* 2019;5:46–65.
- Cancer Genome Atlas Research Network. Comprehensive genomic characterization defines human glioblastoma genes and core pathways. *Nature* 2008;455:1061–8.
- Brennan CW, Verhaak RG, McKenna A, Campos B, Nounshmehr H, Salama SR, et al. The somatic genomic landscape of glioblastoma. *Cell* 2013;155:462–77.
- Fang BA, Kovačević Z, Park KC, Kalinowski DS, Jansson PJ, Lane DJ, et al. Molecular functions of the iron-regulated metastasis suppressor, NDRG1, and its potential as a molecular target for cancer therapy. *Biochim Biophys Acta* 2014; 1845:1–19.
- Shimono A, Okuda T, Kondoh H. N-myc-dependent repression of *ndr1*, a gene identified by direct subtraction of whole mouse embryo cDNAs between wild type and N-myc mutant. *Mech Dev* 1999;83:39–52.
- Kalaydjieva L, Gresham D, Gooding R, Heather L, Baas F, de Jonge R, et al. N-myc downstream-regulated gene 1 is mutated in hereditary motor and sensory neuropathy-Lom. *Am J Hum Genet* 2000;67:47–58.
- Ulrix W, Swinnen JV, Heyns W, Verhoeven G. The differentiation-related gene 1, *Drg1*, is markedly upregulated by androgens in LNCaP prostatic adenocarcinoma cells. *FEBS Lett* 1999;455:23–6.
- Chen B, Nelson DM, Sadovsky Y. N-myc down-regulated gene 1 modulates the response of term human trophoblasts to hypoxic injury. *J Biol Chem* 2006;281: 2764–72.
- Taketomi Y, Sugiki T, Saito T, Ishii Si, Hisada M, Suzuki-Nishimura T, et al. Identification of NDRG1 as an early inducible gene during *in vitro* maturation of cultured mast cells. *Biochem Biophys Res Commun* 2003;306:339–46.
- Watari K, Shibata T, Nabeshima H, Shinoda A, Fukunaga Y, Kawahara A, et al. Impaired differentiation of macrophage lineage cells attenuates bone remodeling and inflammatory angiogenesis in *Ndr1* deficient mice. *Sci Rep* 2016;6:19470.
- Kyuno J, Fukui A, Michiue T, Asashima M. Identification and characterization of *Xenopus* NDRG1. *Biochem Biophys Res Commun* 2003;309:52–7.
- Wakisaka Y, Furuta A, Masuda K, Morikawa W, Kuwano M, Iwaki T. Cellular distribution of NDRG1 protein in the rat kidney and brain during normal postnatal development. *J Histochem Cytochem* 2003;51:1515–25.
- Maruyama Y, Ono M, Kawahara A, Yokoyama T, Basaki Y, Kage M, et al. Tumor growth suppression in pancreatic cancer by a putative metastasis suppressor gene *Cap43/NDRG1/Drg-1* through modulation of angiogenesis. *Cancer Res* 2006;66:6233–42.
- Hosoi F, Izumi H, Kawahara A, Murakami Y, Kinoshita H, Kage M, et al. N-myc downstream regulated gene 1/Cap43 suppresses tumor growth and angiogenesis of pancreatic cancer through attenuation of inhibitor of kappaB kinase beta expression. *Cancer Res* 2009;69:4983–91.
- Murakami Y, Hosoi F, Izumi H, Maruyama Y, Ureshino H, Watari K, et al. Identification of sites subjected to serine/threonine phosphorylation by SGK1 affecting N-myc downstream-regulated gene 1 (NDRG1)/Cap43-dependent suppression of angiogenic CXC chemokine expression in human pancreatic cancer cells. *Biochem Biophys Res Commun* 2010;396:376–81.
- Murakami Y, Watari K, Shibata T, Uba M, Ureshino H, Kawahara A, et al. N-myc downstream-regulated gene 1 promotes tumor inflammatory angiogenesis through JNK activation and autocrine loop of interleukin-1 $\alpha$  by human gastric cancer cells. *J Biol Chem* 2013;288:25025–37.
- Hirata K, Masuda K, Morikawa W, He JW, Kuraoka A, Kuwano M, et al. N-myc downstream-regulated gene 1 expression in injured sciatic nerves. *Glia* 2004;47: 325–34.
- Fukahori S, Yano H, Tsuneoka M, Tanaka Y, Yagi M, Kuwano M, et al. Immunohistochemical expressions of Cap43 and Mina53 proteins in neuroblastoma. *J Pediatr Surg* 2007;42:1831–40.
- Sun B, Chu D, Li W, Chu X, Li Y, Wei D, et al. Decreased expression of NDRG1 in glioma is related to tumor progression and survival of patients. *J Neurooncol* 2009;94:213–9.
- Blaes J, Weiler M, Sahm F, Hentschel B, Osswald M, Czabanka M, et al. NDRG1 prognosticates the natural course of disease in WHO grade II glioma. *J Neurooncol* 2014;117:25–32.
- Weiler M, Blaes J, Pusch S, Sahm F, Czabanka M, Luger S, et al. mTOR target NDRG1 confers MGMT-dependent resistance to alkylating chemotherapy. *Proc Natl Acad Sci U S A* 2014;111:409–14.
- Wakimoto H, Kesari S, Farrell CJ, Curry WT Jr, Zaupa C, Aghi M, et al. Human glioblastoma-derived cancer stem cells: establishment of invasive glioma models and treatment with oncolytic herpes simplex virus vectors. *Cancer Res* 2009;69: 3472–81.
- Wakimoto H, Mohapatra G, Kanai R, Curry WT Jr, Yip S, Nitta M, et al. Maintenance of primary tumor phenotype and genotype in glioblastoma stem cells. *Neuro Oncol* 2012;14:132–44.
- Takahashi-Yanaga F, Yoshihara T, Jingushi K, Igawa K, Tomooka K, Watanabe Y, et al. DIF-1 inhibits tumor growth *in vivo* reducing phosphorylation of GSK-3 $\beta$  and expressions of cyclin D1 and TCF7L2 in cancer model mice. *Biochem Pharmacol* 2014;89:340–8.
- Ishii N, Maier D, Merlo A, Tada M, Sawamura Y, Diserens AC, et al. Frequent co-alterations of TP53, p16/CDKN2A, p14ARF, PTEN tumor suppressor genes in human glioma cell lines. *Brain Pathol* 1999;9:469–79.
- Ma W, Na M, Tang C, Wang H, Lin Z. Overexpression of N-myc downstream-regulated gene 1 inhibits human glioma proliferation and invasion via phosphoinositide 3-kinase/AKT pathways. *Mol Med Rep* 2015;12:1050–8.
- Peifer M, Pai LM, Casey M. Phosphorylation of the *Drosophila* adherens junction protein armadillo: roles for wingless signal and zeste-white 3 kinase. *Dev Biol* 1994;166:543–56.
- Murray JT, Campbell DG, Morrice N, Auld GC, Shpiro N, Marquez R, et al. Exploitation of KESTREL to identify NDRG family members as physiological substrates for SGK1 and GSK3. *Biochem J* 2004;384:477–88.
- Asghar U, Witkiewicz AK, Turner NC, Knudsen ES. The history and future of targeting cyclin-dependent kinases in cancer therapy. *Nat Rev Drug Discov* 2015; 14:130–46.
- Fei D, Xingya C, Da M. Hsp90 maintains the stability and function of the tau phosphorylating kinase GSK3 $\beta$ . *Int J Mol Sci* 2007;8:51–60.
- Failor KL, Desyatnikov Y, Finger LA, Firestone GL. Glucocorticoid-induced degradation of glycogen synthase kinase-3 protein is triggered by serum- and glucocorticoid-induced protein kinase and Akt signaling and controls beta-catenin dynamics and tight junction formation in mammary epithelial tumor cells. *Mol Endocrinol* 2007;21:2403–15.
- Inglis SK, Gallacher M, Brown SG, McTavish N, Getty J, Husband EM, et al. SGK1 activity in Na<sup>+</sup> absorbing airway epithelial cells monitored by assaying NDRG1-Thr346/356/366 phosphorylation. *Pflugers Arch* 2009;457:1287–301.

## Ito et al.

34. Hoang B, Frost P, Shi Y, Belanger E, Benavides A, Pezeshkpour G, et al. Targeting TORC2 in multiple myeloma with a new mTOR kinase inhibitor. *Blood* 2010; 116:4560–8.
35. Morris HR, Taylor GW, Masento MS, Jermyn KA, Kay RR. Chemical structure of the morphogen differentiation inducing factor from *Dictyostelium discoideum*. *Nature* 1987;328:811–4.
36. Arioka M, Takahashi-Yanaga F, Kubo M, Igawa K, Tomooka K, Sasaguri T. Anti-tumor effects of differentiation-inducing factor-1 in malignant melanoma: GSK-3-mediated inhibition of cell proliferation and GSK-3-independent suppression of cell migration and invasion. *Biochem Pharmacol* 2017;138:31–48.
37. Wakimoto H, Tanaka S, Curry WT, Loebel F, Zhao D, Tateishi K, et al. Targetable signaling pathway mutations are associated with malignant phenotype in IDH-mutant gliomas. *Clin Cancer Res* 2014;20:2898–909.
38. Higuchi F, Fink AL, Kiyokawa J, Miller JJ, Koerner MVA, Cahill DP, et al. PLK1 inhibition targets myc-activated malignant glioma cells irrespective of mismatch repair deficiency-mediated acquired resistance to temozolomide. *Mol Cancer Ther* 2018;17:2551–63.
39. Hermida MA, Dinesh Kumar J, Leslie NR. GSK3 and its interactions with the PI3K/AKT/mTOR signalling network. *Adv Biol Regul* 2017;65:5–15.
40. Walz A, Ugolkov A, Chandra S, Kozikowski A, Carneiro BA, O'Halloran TV, et al. Molecular pathways: revisiting glycogen synthase kinase-3 $\beta$  as a target for the treatment of cancer. *Clin Cancer Res* 2017;23:1891–7.
41. Nagini S, Sophia J, Mishra R. Glycogen synthase kinases: moonlighting proteins with theranostic potential in cancer. *Semin Cancer Biol* 2019;56: 25–36.
42. Zhou A, Lin K, Zhang S, Chen Y, Zhang N, Xue J, et al. Nuclear GSK3 $\beta$  promotes tumorigenesis by phosphorylating KDM1A and inducing its deubiquitylation by USP22. *Nat Cell Biol* 2016;18:954–66.
43. Domoto T, Pyko IV, Furuta T, Miyashita K, Uehara M, Shimasaki T, et al. Glycogen synthase kinase-3 $\beta$  is a pivotal mediator of cancer invasion and resistance to therapy. *Cancer Sci* 2016;107:1363–72.
44. Gasser JA, Inuzuka H, Lau AW, Wei W, Beroukhim R, Tokar A. SGK3 mediates INPP4B-dependent PI3K signaling in breast cancer. *Mol Cell* 2014;56:595–607.
45. Gao J, Aksoy BA, Dogrusoz U, Dresdner G, Gross B, Sumer SO, et al. Integrative analysis of complex cancer genomics and clinical profiles using the cBioPortal. *Sci Signal* 2013;6:pl1.
46. Cerami E, Gao J, Dogrusoz U, Gross BE, Sumer SO, Aksoy BA, et al. The cBio cancer genomics portal: an open platform for exploring multidimensional cancer genomics data. *Cancer Discov* 2012;2:401–4.
47. Jingushi K, Takahashi-Yanaga F, Yoshihara T, Shiraishi F, Watanabe Y, Hirata M, et al. DIF-1 inhibits the Wnt/ $\beta$ -catenin signaling pathway by inhibiting TCF7L2 expression in colon cancer cell lines. *Biochem Pharmacol* 2012;83:47–56.
48. Rickman DS, Schulte JH, Eilers M. The expanding world of N-MYC-driven tumors. *Cancer Discov* 2018;8:150–63.
49. Li J, Kretzner L. The growth-inhibitory *Ndr1* gene is a Myc negative target in human neuroblastomas and other cell types with overexpressed N- or c-myc. *Mol Cell Biochem* 2003;250:91–105.
50. Wang J, Wang H, Li Z, Wu Q, Lathia JD, McLendon RE, et al. c-Myc is required for maintenance of glioma cancer stem cells. *PLoS One* 2008;3:e3769.

# Cancer Research

The Journal of Cancer Research (1916–1930) | The American Journal of Cancer (1931–1940)

## Bidirectional Regulation between NDRG1 and GSK3 $\beta$ Controls Tumor Growth and Is Targeted by Differentiation Inducing Factor-1 in Glioblastoma

Hiroshi Ito, Kosuke Watari, Tomohiro Shibata, et al.

*Cancer Res* 2020;80:234-248. Published OnlineFirst November 13, 2019.

<b>Updated version</b>	Access the most recent version of this article at: doi: <a href="https://doi.org/10.1158/0008-5472.CAN-19-0438">10.1158/0008-5472.CAN-19-0438</a>
<b>Supplementary Material</b>	Access the most recent supplemental material at: <a href="http://cancerres.aacrjournals.org/content/suppl/2019/11/13/0008-5472.CAN-19-0438.DC1">http://cancerres.aacrjournals.org/content/suppl/2019/11/13/0008-5472.CAN-19-0438.DC1</a>

<b>Cited articles</b>	This article cites 50 articles, 14 of which you can access for free at: <a href="http://cancerres.aacrjournals.org/content/80/2/234.full#ref-list-1">http://cancerres.aacrjournals.org/content/80/2/234.full#ref-list-1</a>
-----------------------	--

<b>E-mail alerts</b>	<a href="#">Sign up to receive free email-alerts</a> related to this article or journal.
<b>Reprints and Subscriptions</b>	To order reprints of this article or to subscribe to the journal, contact the AACR Publications Department at <a href="mailto:pubs@aacr.org">pubs@aacr.org</a> .
<b>Permissions</b>	To request permission to re-use all or part of this article, use this link <a href="http://cancerres.aacrjournals.org/content/80/2/234">http://cancerres.aacrjournals.org/content/80/2/234</a> . Click on "Request Permissions" which will take you to the Copyright Clearance Center's (CCC) Rightslink site.